

First principles calculation of vibrational Raman spectra in large systems: signature of small rings in crystalline SiO₂

Michele Lazzeri and Francesco Mauri

Laboratoire de Minéralogie Cristallographie de Paris, 4 Place Jussieu, 75252 Paris cedex 05, France.

(Dated: March 22, 2022)

We present an approach for the efficient calculation of vibrational Raman intensities in periodic systems within density functional theory. The Raman intensities are computed from the second order derivative of the electronic density matrix with respect to a uniform electric field. In contrast to previous approaches, the computational effort required by our method for the evaluation of the intensities is negligible compared to that required for the calculation of vibrational frequencies. As a first application, we study the signature of 3- and 4-membered rings in the the Raman spectra of several polymorphs of SiO₂, including a zeolite having 102 atoms per unit cell.

PACS numbers: 71.15.-m, 78.30.-j, 71.15.Mb

Vibrational Raman spectroscopy [1] is one of the most widely used optical techniques in materials science. It is a standard method for quality control in production lines. It is very effective in determining the occurrence of new phases or structural changes at extreme conditions (high pressure and temperature), where it is often preferred to the more difficult and less readily available x-ray diffraction experiments based on synchrotron sources [2]. Moreover, it can be used in the absence of long-range structural order as for liquid or amorphous materials [3, 4, 5]. The theoretical determination of Raman spectra is highly desirable, since it can be used to associate Raman lines to specific microscopic structures.

Density functional theory (DFT) [6] can be used to determine with high accuracy both frequencies and intensities of Raman spectra. Vibrational frequencies can be efficiently determined using *first order response* [7, 8]. Within this approach Raman intensities (RI) calculation is also possible, but requires a computational time significantly larger and is not practical for large systems. Thus, while many examples of frequency calculations have been reported so far [7], RI were predicted from first-principles in a very limited number of cases involving systems with a small number of atoms [9, 10, 11]. In this Letter we show that it is possible to obtain RI in extended solids with a computational cost negligible with respect to that required for the frequency determination. The efficiency of our approach will lead *ab-initio* calculations to become a routine instrument for the interpretation of experimental Raman data. Our method is based on *second order response* to DFT. In particular, we compute the second order derivative of the electronic density matrix with respect to a uniform electric field, using pseudopotentials and periodic boundary conditions. As a first application we calculate Raman spectra of several SiO₂ polymorphs, including a zeolite having 102 atoms per unit cell [12].

In a Raman spectrum the peak positions are fixed by the frequencies ω_ν of the optical phonons with null wavevector. In non-resonant Stokes Raman spectra of

harmonic solids, the peak intensities I^ν can be computed within the Placzek approximation [1] as:

$$I^\nu \propto |\mathbf{e}_i \cdot \vec{\mathbf{A}}^\nu \cdot \mathbf{e}_s|^2 \frac{1}{\omega_\nu} (n_\nu + 1), \quad (1)$$

where \mathbf{e}_i (\mathbf{e}_s) is the polarization of the incident (scattered) radiation, $n_\nu = (\exp(\hbar\omega_\nu/k_B T) - 1)^{-1}$, T is the temperature, and

$$A_{lm}^\nu = \sum_{k\gamma} \frac{\partial^3 \mathcal{E}^{\text{el}}}{\partial E_l \partial E_m \partial u_{k\gamma}} \frac{w_{k\gamma}^\nu}{\sqrt{M_\gamma}}. \quad (2)$$

Here \mathcal{E}^{el} is the electronic energy of the system, E_l is the l^{th} Cartesian component of a uniform electric field, $u_{k\gamma}$ is the displacement of the γ^{th} atom in the k^{th} direction, M_γ is the atomic mass, and $w_{k\gamma}^\nu$ is the orthonormal vibrational eigenmode ν .

Linear response [7, 8] can be used to determine ω_ν , \mathbf{w}^ν , and also the dielectric tensor $\vec{\epsilon}^\infty$ defined as $\epsilon_{lm}^\infty = \delta_{lm} - (4\pi/\Omega) \partial^2 \mathcal{E}^{\text{el}} / (\partial E_l \partial E_m)$, where Ω is the cell volume. RI have been computed [9, 10] through Eq. (1), obtaining $\vec{\mathbf{A}}^\nu$ by finite-differences derivation of $\vec{\epsilon}^\infty$ with respect $u_{k\gamma}$. This approach requires $36N^{\text{at}}$ linear response calculations, where N^{at} is the number of atoms. Thus, the scaling of the RI calculation is the same as that of the frequency calculation with a much larger prefactor. This has limited the applications of this approach to small systems. RI have also been computed from the dynamical autocorrelation functions of $\vec{\epsilon}^\infty$ in a molecular dynamics (MD) run [11]. This approach also copes with liquids or anharmonic solids, but is very demanding, requiring the calculation of $\vec{\epsilon}^\infty$ at each MD step.

Alternatively, RI can be obtained knowing the second order derivative of the DFT density matrix $\rho = \sum_v |\psi_v\rangle \langle \psi_v|$, being $|\psi_v\rangle$ the normalized occupied Kohn-Sham (KS) eigenstates [6]. In fact, according to the well known Hellmann-Feynman theorem

$$\frac{\partial \mathcal{E}^{\text{el}}}{\partial u_{k\gamma}} = 2 \text{Tr} \left\{ \rho \frac{\partial v^{\text{ext}}}{\partial u_{k\gamma}} \right\},$$

where $\text{Tr}\{O\}$ is the trace of the operator O , and v^{ext} is the external ionic potential (the KS self-consistent potential is $V^{\text{KS}} = V^{\text{Hxc}} + v^{\text{ext}}$, where V^{Hxc} is the sum of the Hartree and the exchange-correlation potential). Thus

$$\frac{\partial^3 \mathcal{E}^{\text{el}}}{\partial E_l \partial E_m \partial u_{k\gamma}} = 2 \text{Tr} \left\{ \left(\frac{\partial^2 \rho}{\partial E_l \partial E_m} \right) \frac{\partial v^{\text{ext}}}{\partial u_{k\gamma}} \right\}. \quad (3)$$

The $\partial^2 \rho / (\partial E_l \partial E_m)$ calculation requires six second-order calculations, instead of the $36N^{\text{at}}$ first-order calculations needed for the finite-differentiation [10]. Because of this better size-scaling, the $\hat{\mathbf{A}}^\nu$ calculation through Eq. (3) is much more efficient and the time for RI calculation is negligible compared to that for ω_ν in large systems.

The approach based on Eq. (3) has already been used in isolated molecules [13] but never in extended systems. Indeed, in solids the calculation of $\partial^2 \rho / (\partial E_l \partial E_m)$ is not trivial because the position operator, required by the electric field perturbation, is ill-defined in periodic boundary conditions. Because of this, although a formalism to calculate derivatives of ρ at any order was proposed by Gonze already in 1995 [8], only very recently Nunes and Gonze [14] were able to include perturbations due to macroscopic electric fields. To do that, they use the polarization-Berry phase formalism [15], arguing that this concept remains valid in the presence of finite electric fields. This approach has been applied so far to a one dimensional non-self-consistent model [14]. In the following we give an expression for the second derivative of ρ , that does not require the Berry phase formalism to cope with uniform electric fields, and we use it to compute $\hat{\mathbf{A}}^\nu$ in real systems with a DFT self-consistent Hamiltonian.

The derivative of ρ with respect to two generic perturbation parameters λ and μ is:

$$\begin{aligned} \frac{\partial^2 \rho}{\partial \lambda \partial \mu} = & \sum_v \left(|P \eta_v^{(\lambda, \mu)}\rangle \langle \psi_v| + |P \frac{\partial \psi_v}{\partial \lambda}\rangle \langle \frac{\partial \psi_v}{\partial \mu} P| + \right. \\ & \left. - \sum_{v'} |\psi_{v'}\rangle \langle \frac{\partial \psi_{v'}}{\partial \lambda} P| P \frac{\partial \psi_v}{\partial \mu} \rangle \langle \psi_v| \right) + cc, \quad (4) \end{aligned}$$

where $P = (\mathbf{1} - \rho)$ is the projector on the empty state subspace, the sums over v and v' run over the occupied states, and $|\eta_v^{(\lambda, \mu)}\rangle$ are the second derivatives of the occupied KS-orbitals in the parallel-transport gauge [8]. According to our derivation:

$$|P \frac{\partial \psi_v}{\partial \lambda}\rangle = \tilde{G}_v \left[\frac{\partial V^{\text{KS}}}{\partial \lambda}, \rho \right] |\psi_v\rangle, \quad (5)$$

$$\begin{aligned} |P \eta_v^{(\lambda, \mu)}\rangle = & \tilde{G}_v \left\{ \frac{\partial^2 V^{\text{KS}}}{\partial \lambda \partial \mu} + \left[\frac{\partial V^{\text{KS}}}{\partial \lambda}, \frac{\partial \rho}{\partial \mu} \right] + \right. \\ & \left. + \left[\frac{\partial V^{\text{KS}}}{\partial \mu}, \frac{\partial \rho}{\partial \lambda} \right] \right\} |\psi_v\rangle. \quad (6) \end{aligned}$$

Here,

$$\tilde{G}_v = \sum_c \frac{|\psi_c\rangle \langle \psi_c|}{\epsilon_v - \epsilon_c}$$

TABLE I: Raman activity in Si computed with our approach (γ_{SOR}), and by finite differences (γ_{FD}). N is the number of inequivalent k-points.

N	2	10	28	60	110	182
γ_{SOR}	8.54	5.30	5.32	5.39	5.40	5.40
γ_{FD}	18.99	7.09	5.69	5.45	5.41	5.40
γ_{FD} Ref. [9]		7.10				

is the Green function operator projected on the empty states $|\psi_c\rangle$ [16], $[A, B] = AB - BA$, and the first derivative of the density matrix is:

$$\frac{\partial \rho}{\partial \mu} = \sum_v |P \frac{\partial \psi_v}{\partial \mu}\rangle \langle \psi_v| + cc. \quad (7)$$

Since $\partial V^{\text{KS}} / \partial \lambda$ and $\partial^2 V^{\text{KS}} / (\partial \lambda \partial \mu)$ depend on $\partial \rho / \partial \lambda$, $\partial \rho / \partial \mu$, and $\partial^2 \rho / (\partial \lambda \partial \mu)$, Eqs. (4-7), should be solved self-consistently.

The advantage of the present formulation, compared to that of Ref. [8], lies in the introduction of the commutators of Eqs. (5,6). Thanks to the commutators, all the quantities needed with our formalism are well defined in an extended insulator, even if the perturbation μ or λ are the component E_l of a uniform electric field, i.e. if $\partial V^{\text{KS}} / \partial \lambda = -er_l + \partial V^{\text{Hxc}} / \partial E_l$ [17], being r_l the l^{th} Cartesian component of the position operator \mathbf{r} , and e the electron charge. In particular, in an insulator, the commutators $[\mathbf{r}, \rho]$ and $[\mathbf{r}, \partial \rho / \partial \mu]$ in Eqs. (5,6) are well defined, bounded operators, since the density matrix is localized ($\langle \mathbf{r}'' | \rho | \mathbf{r}' \rangle$ goes to zero exponentially for $|\mathbf{r}'' - \mathbf{r}'| \rightarrow \infty$).

Finally, in a periodic system, the right-hand side of Eq. (6) can be easily computed in terms of the $|u_i^{\mathbf{k}}\rangle$, that are the periodic parts of the Bloch-wavefunctions $|\psi_i^{\mathbf{k}}\rangle$ with reciprocal-lattice vector \mathbf{k} , using the substitutions:

$$\langle \psi_c^{\mathbf{k}} | [r_l, \rho] | \psi_v^{\mathbf{k}} \rangle = i \sum_{v'} \langle u_c^{\mathbf{k}} | \frac{\partial |u_{v'}^{\mathbf{k}}\rangle \langle u_{v'}^{\mathbf{k}}|}{\partial k_l} | u_v^{\mathbf{k}} \rangle \quad (8)$$

$$\langle \psi_c^{\mathbf{k}} | \left[r_l, \frac{\partial \rho}{\partial E_m} \right] | \psi_v^{\mathbf{k}} \rangle = i \sum_{v'} \langle u_c^{\mathbf{k}} | \frac{\partial |P_{\mathbf{k}} \frac{\partial u_{v'}^{\mathbf{k}}}{\partial E_m}\rangle \langle u_{v'}^{\mathbf{k}}|}{\partial k_l} | u_v^{\mathbf{k}} \rangle \quad (9)$$

where l and m are Cartesian indexes, c is an empty band index, v and v' are occupied band indexes, and $P_{\mathbf{k}}$ is the projector on the empty subspace of the point \mathbf{k} . In our implementation, the derivative with respect to k_l in the right-hand side of Eq. (9) is computed numerically by finite-differences, using an expression independent from the arbitrary wavefunction-phase, as in Refs. [14, 18].

We test our approach on Si in the diamond phase, where the Raman activity is determined by $\gamma = a \partial \epsilon_{11}^{\infty} / \partial u$ [9], where $a = 10.20 \text{ a.u.}$ is the lattice spacing and u the displacement of one atom along the $(1, 1, 1)$ direction [19]. We compute γ for various grids of k-points, using both our second order response method (γ_{SOR}) and by finite

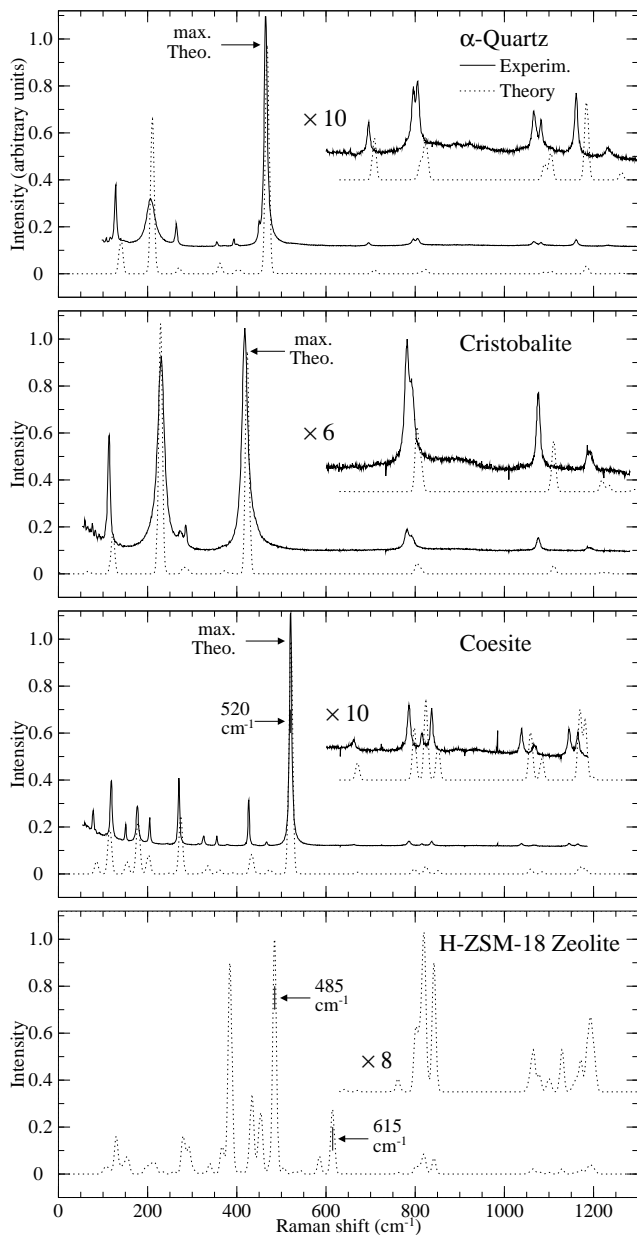


FIG. 1: Vibrational Raman spectra of various SiO_2 polymorph powders. Measurements are from Refs. [22]. Theoretical frequencies are rescaled by +5%, and the spectra are convoluted with a uniform Gaussian broadening having 4.0 cm^{-1} width.

differentiation with respect to the atomic displacement (γ_{FD}), Tab. I. At convergence the two approaches are completely equivalent.

As a second application, we consider tetrahedral SiO_2 . In this class of materials, that includes the all-silica zeolites, the quartz, cristobalite, tridymite and coesite polymorphs of SiO_2 , and vitreous silica ($v\text{-SiO}_2$), each Si atom is tetrahedrally coordinated to four O atoms and each O atom is bonded to two Si atoms. The properties of these systems can be effectively described in terms of

the n -membered rings (n -MRs) of tetrahedra contained in their structure [3, 4, 5]. E.g., a clear correlation between the presence of 3- and 4-MRs and the degradation of optical $v\text{-SiO}_2$ fibers under UV radiation has been observed [4]. In the $v\text{-SiO}_2$ Raman spectra the two sharp peaks at 490 cm^{-1} (D_1 line) and 606 cm^{-1} (D_2 line), have been attributed to the breathing mode (BM) of the O atoms towards the ring center of 4-MRs and 3-MRs, respectively [3]. This attribution has been confirmed by DFT vibrational frequency calculations [5]. The attribution would be further supported by experimental measurements on well characterized crystalline polymorphs containing 3- and 4-MRs. However, the strong Raman peak at 520 cm^{-1} in coesite, a phase that contains 4-MRs, is shifted by 30 cm^{-1} with respect to the D_1 line in $v\text{-SiO}_2$, and no Raman measurements has been published on the H-ZSM-18 zeolite, that is the only known SiO_2 crystalline polymorph with 3-MRs [12]. Interestingly this zeolite contains 4-MRs as well.

To clarify this topic, we compute the Raman spectra of α -quartz, coesite, α -cristobalite, and H-ZSM-18 [19, 20]. In Fig. 1, we compare our results with the available experimental spectra [22]. The vibrational frequencies are systematically underestimated by 5% by our calculation. To simplify the comparison with the experiments, in Fig. 1 and 2, the theoretical frequencies are multiplied by a scaling factor of 1.05. The ability of the method in reproducing quantitatively all the measured features is evident.

In order to associate Raman peaks of Fig. 1 to the small-ring BMs, we project the vibrational eigenmode \vec{w}^ν on the subspace generated by the BMs of a given kind of rings, \mathcal{R} , and on the corresponding complementary subspace, $\bar{\mathcal{R}}$. We use the two resulting projected vectors to decompose \vec{A}^ν so that $\vec{A}^\nu = \vec{A}_{\mathcal{R}}^\nu + \vec{A}_{\bar{\mathcal{R}}}^\nu$. Since I^ν is quadratic in \vec{A}^ν , see Eq. (1), $I^\nu = I_{\mathcal{R}}^\nu + I_{\bar{\mathcal{R}}}^\nu + I_{\text{overlap}}^\nu$, where I_{overlap}^ν is the term bilinear in $\vec{A}_{\mathcal{R}}^\nu$ and $\vec{A}_{\bar{\mathcal{R}}}^\nu$. A Raman peak can be associated to a ring BM (i.e. the Raman activity is solely due to the BM) if, and only if, $I_{\mathcal{R}}^\nu \gg |I_{\text{overlap}}^\nu|$.

The structure of H-ZSM-18 [12] contains two equivalent 3-MRs and two kinds of 4-MRs which we will call 4-MRs_0 , and 4-MRs_1 [23]. In Fig. 2, we show the projected Raman spectra of the zeolite and the coesite. In the H-ZSM-18 spectrum, the peaks at 485, and 615 cm^{-1} are very well described by the BM of 4-MRs_0 and 3-MRs, respectively. A direct analysis of the vibrational eigenmodes shows that both BMs are decoupled from other modes. The frequencies of the two peaks are very close to those of the measured D_1 and D_2 lines in $v\text{-SiO}_2$ (490 , and 606 cm^{-1}), thus confirming that these lines are due to rings BMs [3, 5]. However, the presence of small-MRs in a structure does not guarantee, in general, the occurrence of completely decoupled BMs. This is the case of the 4-MRs in coesite and the 4-MRs_1 in the zeolite, whose BMs exhibit a large $|I_{\text{overlap}}^\nu|$, see Fig. 2. These over-

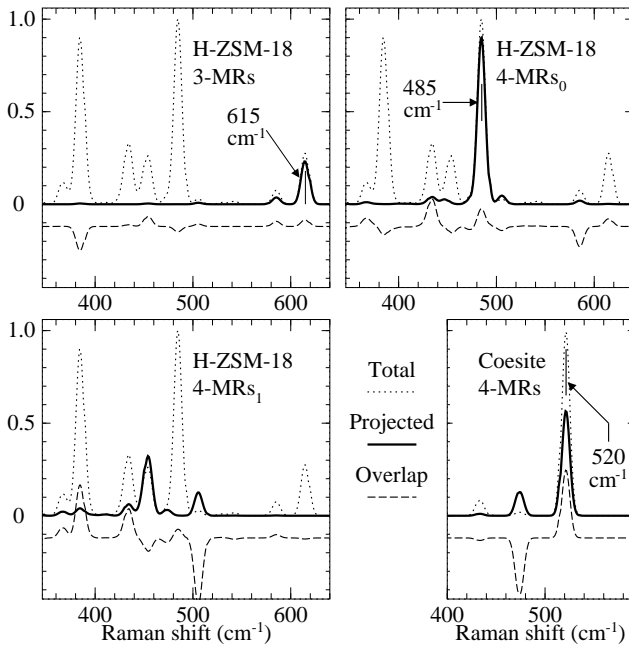


FIG. 2: Raman intensities projected on the breathing modes of various rings labeled 3-MRs, and 4-MRs_x (see the text). For clarity, the overlap intensity (I_{overlap}^{ν} in the text) is shifted vertically.

laps imply the existence of a coupling with other modes, that, in turn, explains the 30 cm^{-1} difference between the 4-MRs frequency of coesite and that of the D_1 line of $\nu\text{-SiO}_2$. A comparable frequency shift from the D_1 line is observed, with opposite sign, for the 4-MRs₁ BMs in the zeolite.

In conclusion, with the aim of building an instrument for the routine interpretation of Raman spectra, we developed a method for the efficient calculation of Raman intensity. We computed the Raman spectra of SiO_2 polymorphs containing up to 102 atoms. We found that: i) not all the small-membered-rings have decoupled breathing modes, ii) the H-ZSM-18 zeolite provides decoupled breathing mode of 4- and 3-membered rings, whose frequencies nicely coincide with the D_1 and D_2 lines of vitreous silica. An experimental determination of the Raman spectra of this zeolite can thus provide an experimental calibration for the determination of the density of decoupled small membered rings in vitreous silica.

Calculations were performed at IDRIS supercomputing center. Our approach was implemented in the PWSCF code [24].

in *Mineralogy*, vol. 37: *Ultra-high Pressure Mineralogy*, Edited by R.J. Hemley (Mineralogical Society of America, Washington DC, 1998) p. 525.

- [3] S.K. Sharma, J.F. Mammone, and M.F. Nicol, *Nature* **292**, 140 (1981).
- [4] H. Hosono *et al.*, *Phys. Rev. Lett.* **87**, 175501 (2001).
- [5] A. Pasquarello and R. Car, *Phys. Rev. Lett.* **80**, 5145 (1998). F.L. Galeener *et al.*, *Phys. Rev. Lett.* **53**, 2429 (1984).
- [6] P. Hohenberg and W. Kohn, *Phys. Rev.* **136B**, 864 (1964); W. Kohn and L.J. Sham, *Phys. Rev.* **140A**, 1133 (1965).
- [7] P. Giannozzi *et al.*, *Phys. Rev. B* **43**, 7231 (1991); S. Baroni *et al.*, *Rev. Mod. Phys.* **73**, 515 (2001); X. Gonze, C. Lee, *Phys. Rev. B* **55**, 10355 (1997).
- [8] X. Gonze, *Phys. Rev. A* **52**, 1096 (1995). Note that the term depending on the Lagrange multipliers should not be omitted in the derivation of Eq. (55) from Eq. (54).
- [9] S. Baroni and R. Resta, *Phys. Rev. B* **33**, 5969 (1986).
- [10] P. Umari, A. Pasquarello, and A. Dal Corso, *Phys. Rev. B* **63**, 094305 (2001).
- [11] A. Putrino and M. Parrinello, *Phys. Rev. Lett.* **88**, 176401 (2002).
- [12] S.L. Lawton and W.J. Rohrbaugh, *Science* **247**, 1319 (1990).
- [13] M.J. Frisch *et al.*, *J. Chem. Phys.* **84**, 531 (1986).
- [14] R.W. Nunes and X. Gonze, *Phys. Rev. B* **63**, 155107 (2001).
- [15] R.D. King-Smith and D. Vanderbilt, *Phys. Rev. B* **47**, 1651 (1993).
- [16] The operator \tilde{G}_v can be efficiently applied to any vector by solving a linear system, following Refs. [7, 8].
- [17] Since we are interested in a perturbation with respect to the *macroscopic* uniform electric field, we set to zero the uniform component of the Hartree potential in $\partial V^{\text{Hxc}}/\partial E_l$ and in $\partial^2 V^{\text{Hxc}}/\partial E_l \partial E_m$ [7].
- [18] A. Dal Corso and F. Mauri, *Phys. Rev. B* **50**, 5756 (1994).
- [19] We use the local density approximation, norm conserving pseudopotential [N. Trouiller and J.L. Martins, *Phys. Rev. B* **43**, 1993 (1991)] and we expand the wavefunctions in plane-wave with a cutoff of 25 and 60 Ry, in Si and SiO_2 systems, respectively.
- [20] We use the experimental lattice constants [12, 21], 1 special k-point for H-ZSM-18, and 3 k-points in the other systems. Internal coordinates are relaxed by energy minimization. Raman spectra are computed in backscattering geometry taking into account the TO-LO splitting of the frequencies [7].
- [21] G. Will *et al.*, *J. Appl. Cryst.* **21**, 182 (1988). K.L. Geisinger *et al.*, *J. Phys. Chem.* **91**, 3237 (1987). W.W. Schmahl *et al.*, *Z. Kristallogr.* **201**, 125 (1992).
- [22] Handbook of Minerals Raman Spectra, <http://www.ens-lyon.fr/LST/Raman>. See also P. Gillet, A. Le Cleach, and M. Madon, *J. Geophys. Res.*, **95**, 21635 (1990); K.J. Kingma, R.J. Hemley, *Am. Mineral.* **79**, 269, (1994).
- [23] In a unit cell, there are twelve equivalent 4-MRs₀, which are joined in four groups of three. In each group the three rings are sharing one Si atom. There are six equivalent 4-MRs₁ which are disjointed between them.
- [24] S. Baroni, A. Dal Corso, S. de Gironcoli, and P. Giannozzi, <http://www.pwscf.org>.

[1] P. Brüesch, *Phonons: Theory and Experiments II* (Springer, Berlin, 1986).

[2] P. Gillet, R.J. Hemley, and P.F. Mc Millan, *Reviews*